Proton Character of the Peptide Unit in the Ca^{2+}-Binding Sites of Calcium Pump

Huifang Li,[†] Yuxiang Bu,*[,†,‡,§] Shihai Yan,[†] Ping Li,[†,‡] and Robert I. Cukier[§]

School of Chemistry, Qufu Normal University, Qufu, 273165, PRC, Institute of Theoretical Chemistry, Shandong University, Jinan, 250100, PRC, and Department of Chemistry, Michigan State University, East Lansing, Michigan 48824

Received: January 25, 2006; In Final Form: March 22, 2006

The effect of forming calcium pump structures in biological systems on the proton character of the peptide unit has been studied theoretically using the density-functional theory calculations with a large basis set. One acetic acid, one acetate, and three acetamide molecules as well as the modeling peptide unit (MPU) have been employed to mimic the amino acid residues forming the Ca^{2+}-binding sites. To highlight the limiting case of the Ca^{2+}-binding effect on the proton property and the proton countertransport possibility in the direction opposite to the ion, the MPU bounded by the bare or the hydrated Ca^{2+} has also been investigated. The natural bond orbital (NBO) analysis indicates that the increase of the p-character of the (N−H) σ orbital results in weakening of the N−H bond which is lengthened when a Ca^{2+} ion is introduced to the MPU. Calculated NMR shielding σ(H1) of the MPU shifts upfield upon the Ca^{2+} ion combination, which reveals the donating of the electron from the amide H as represented by the increase of the calculated positive natural charge for amide H of the MPU. Moreover, the proton affinities (PA) and gas-phase basicities (GB) for the amide nitrogen active site of the MPU are reduced; that is, the acidity of the amide hydrogen gets stronger because of the influence of the Ca^{2+} ion. To prove the transport possibility of the N−H proton in the direction opposite to the Ca^{2+} ion along the N−H···O═C hydrogen bond in the helical peptide linkage, NH_3 and H_2O are used here to assist the dissociation of the amide H of the MPU, and the calculated results show the notable decrease of the deprotonation energies compared to that of the case without this assistance. Moreover, calculated results also reveal that the variation of the quantities discussed here for amide H of the MPU gets smaller when the acidity of Ca^{2+} ion decreases. Ionization states of the acidic residues forming the Ca^{2+}-binding sites may influence the activity of the amide H of the MPU and further affect the transport tendency of the peptide unit proton in the direction opposite to Ca^{2+}.

1. Introduction

Ca^{2+} is crucial in many biological processes through its interactions with Ca^{2+}-receptor/binding proteins forming calcium pump.[1−7] For example, Ca^{2+} is a fundamental and ubiquitous factor in the regulation of intracellular processes, and it also plays a central role in eukaryotic signal transduction, etc. Therefore, Ca^{2+}-ATPase, which is a member of the P-type ATPases transporting ions across the membrane against a concentration gradient, has been investigated by many workers.[1,2,8−13]

The calcium pump of sarcoplasmic reticulum (SR) Ca^{2+}-ATPase (SERCA) is one of the most representative members of a group of enzymes called P-type ATPases, so called because they are autophosphorylated (at Asp 351 with Ca^{2+}-ATPase) during the reaction cycle. SERCA is an integral membrane protein of relative molecular mass 110 000 (M_r 110K). It pumps Ca^{2+} released in muscle cells during contraction back onto the sarcoplasmic reticulum using the chemical energy of ATP, thereby causing the relaxation of muscle cells, and establishes a concentration gradient of Ca^{2+} across the SR membrane by transporting two Ca^{2+} ions per ATP hydrolyzed.[1,2,14−18]

Recently, X-ray structures of SR Ca^{2+}-ATPase in five different physiological states have revealed that large conformational changes occur during Ca^{2+} transport, and they also provide atomic models for two high-affinity Ca^{2+} binding sites of the peptide linkage in the transmembrane region consisting of 10 helixes (M1−M10).[1,2,19−21] We can know from these X-ray structures (at 2.6 and 2.9 Å resolution[2,19]) that the ionization states of the acetic residues of the peptide linkage forming the binding sites have particular importance since the binding of Ca^{2+} involves a structural rearrangement and the helical peptide linkage structures are distorted. The exposed hydrophobic pocket can then interact with other proteins in the cell, thereby modulating their function.[22] Ca^{2+}-ATPase may influence the activity of the amide H of the peptide unit and transport the proton of the peptide in the direction opposite to Ca^{2+}. This transport process is called the proton countertransport.

At present, relatively little is known at a quantum mechanical (QM) level about the formation of the Ca^{2+} pump that allows Ca^{2+} to induce a proton countertransport of the peptide. Therefore, the proton countertransport of the modeling peptide unit (MPU) in the Ca^{2+}-binding sites of the calcium pump will be studied theoretically using the density-functional theory[23,24] in this work because these cation interactions can be well described using a QM method. Also, the first attempt to use a QM method to predict the effect of Ca^{2+} binding to the MPU via the selected nuclear magnetic resonance (NMR) parameters will be presented because NMR spectroscopy is a potentially powerful tool that has been used during the past decades for the detection of intermolecular interactions,[24,25] and the progress in the QM field has made possible NMR calculations that are

* To whom correspondence should be addressed. E-mail: byx@sdu.edu.cn.
† Qufu Normal University.
‡ Shandong University.
§ Michigan State University.

10.1021/jp060531v CCC: $33.50
Published on Web 05/13/2006

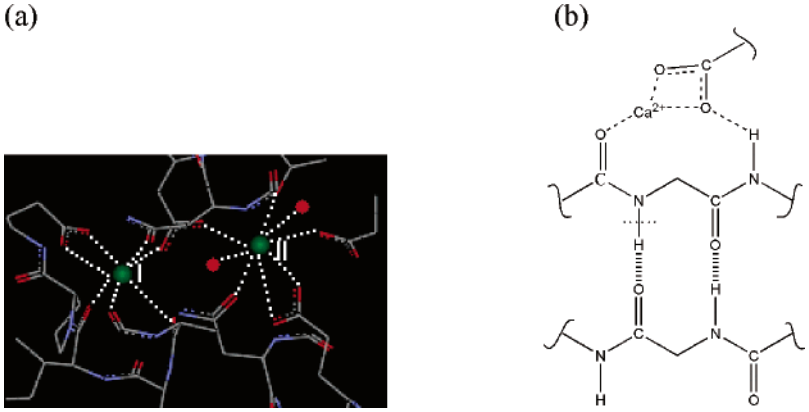

Figure 1. (a) Energy-minimized structure of the Ca^{2+}-binding sites viewed from the cytoplasmic side of SERCA. Ca^{2+} ions are indicated in ball representations in a green color, and red spheres represent water. Dotted lines show the coordination of Ca^{2+} and oxygen atoms. (b) Two-dimensional schematic representation of the cyclic network proton countertransport discussed in the present paper. Slashed lines indicate hydrogen bonds, and other sides of the peptide bonds are indicated by curving lines for simplicity.

useful, accurate, and reliable on biomolecular fragments of considerable size.[24−29]

As shown in Figure 1a, which is abridged from the X-ray SR Ca^{2+}-ATPase structure at the 2.6 Å resolution in the protein database,[2] Ca^{2+} is coordinated by seven carbonyl oxygens of the amino acid residues in both high-affinity Ca^{2+} ions (Figure 1) of the SR Ca^{2+}-ATPase used for our discussion of the proton countertransport. All of the residues on the first shell of the site I of calcium pump have been identified as critical by mutagenesis studies. These residues are four side chain oxygen atoms of Glu309, Asn796, and Asp800 and three backbone carbonyl oxygen atoms of Val304, Ala305, and Ile307, respectively.[30] Calcium pump is simulated, depending on this site I of the Ca^{2+} in the SERCA structure, to investigate the effect of Ca^{2+} on the ionized peptide, especially the activity of the amide H in the Ca^{2+} binding sites of the peptide linkage.

As mentioned above, the ionized states of the acidic residues forming the Ca^{2+} pump of SR Ca^{2+}-ATPase may influence the activity of the amide H of the MPU and further affect the transport tendency of the peptide unit proton in the direction opposite to Ca^{2+}. From the protein structure of Ca^{2+} pump, we know that the N−H···O═C hydrogen bonds of the helical peptide linkage provide proton donor and acceptor groups as shown in Figure 1b.[31] Therefore, we can predict that the proton transfer will happen if there are stronger electron-withdrawing groups, such as carbonyl O of the peptide linkage forming a hydrogen bond with the proton H. To verify our prediction, NH_3 and H_2O are used as the assisting groups for the dissociation of the amide H in the MPU. Although no proton transfer has experimentally been observed from the amide nitrogen of the MPU to other groups up to now, this study may provide some insights into the feasibility of the proton countertransport when SERCA is formed because the Ca^{2+} binding to the peptide unit may significantly affect the property of the proton in the peptide unit.

To our best knowledge, no such theoretical investigations have been reported up to now. Expectedly, this exploration may help to understand what happens regarding the behavior and character of the proton in the peptide linkage when calcium pump is formed.

2. Computational Details

According to the first site (site I) of the abridged X-ray SR Ca^{2+}-ATPase structure shown in Figure 1, one acetic acid, one acetate, and three acetamide groups as well as the MPU have been employed to mimic the amino acid residues to form the Ca^{2+}-binding sites of the peptide linkage, forming the modeling calcium pump (MCP) structure (see Figure 2c). That is, the amino acid residues cluster forming the Ca^{2+}-binding sites are modeled by keeping their active groups and substituting their backbones with $-CH_3$ for simplification of the computation. In the same way, two sides of the backbones of the peptide unit $-CO-NH-$ are substituted by the $-CH_3$ groups for the sake of simplicity, forming the MPU (see Figure 2a). Besides the MCP, the bare or hydrated Ca^{2+} coordinated MPU structures, denoted by CM and (1−6)CM (see Figure 2b), are also analyzed in order to highlight the limiting case of the Ca^{2+} binding effects on the proton countertransport in the direction opposite to the ion. The number of H_2O molecules forming the Ca^{2+} binding sites ranges from one to six because the Ca^{2+} ion is coordinated by seven oxygen atoms in the calcium pump structures.

All of the complexes are fully gradient optimized employing the appropriate DFT method with the B3LYP exchange-correlation functional and the 6-311+G* basis set. Frequency analyses have been made to ascertain the nature of the optimized structures.

The dissociation energy (ΔE_d) for the amide H of the MPU is determined as follows:

$$\Delta E_d = E_{M'} - E_M \tag{1}$$

$$\Delta E_d = (E_{H\cdots A} + E_{M'}) - E_M \tag{2}$$

where the subscript M refers to the total system, $E_{M'}$ indicates the optimized energy of the deprotonated MCP or the MPU with the bare and the hydrated Ca^{2+} ion, and $E_{H\cdots A}$ means the energy of the protonated assisting group (viz., H···H_2O and H···NH_3). Moreover, for these deprotonation processes, that is, $MH \rightarrow M^- + H^+$, the enthalpy changes and Gibbs free energy changes can be calculated as

$$\begin{aligned}\Delta H &= E(MH^+) - E(M) - E(H^+) + \Delta(PV) \\ &= E(MH^+) - E(M) + E'_{vib}(MH^+) - E'_{vib}(M) - 2.5RT\end{aligned} \tag{3}$$

$$\Delta G = \Delta H - T\Delta S \quad \Delta S = S(MH^+) - S(M) - S(H^+)) \tag{4}$$

where the E(i), E'_{vib}(i), and S(i) mean the total energy, zero-point vibrational energy (ZPVE) also including the thermal vibrational corrections to the total energy for simplicity, and entropy of the species i, respectively.[32] As a rule, GB and PA

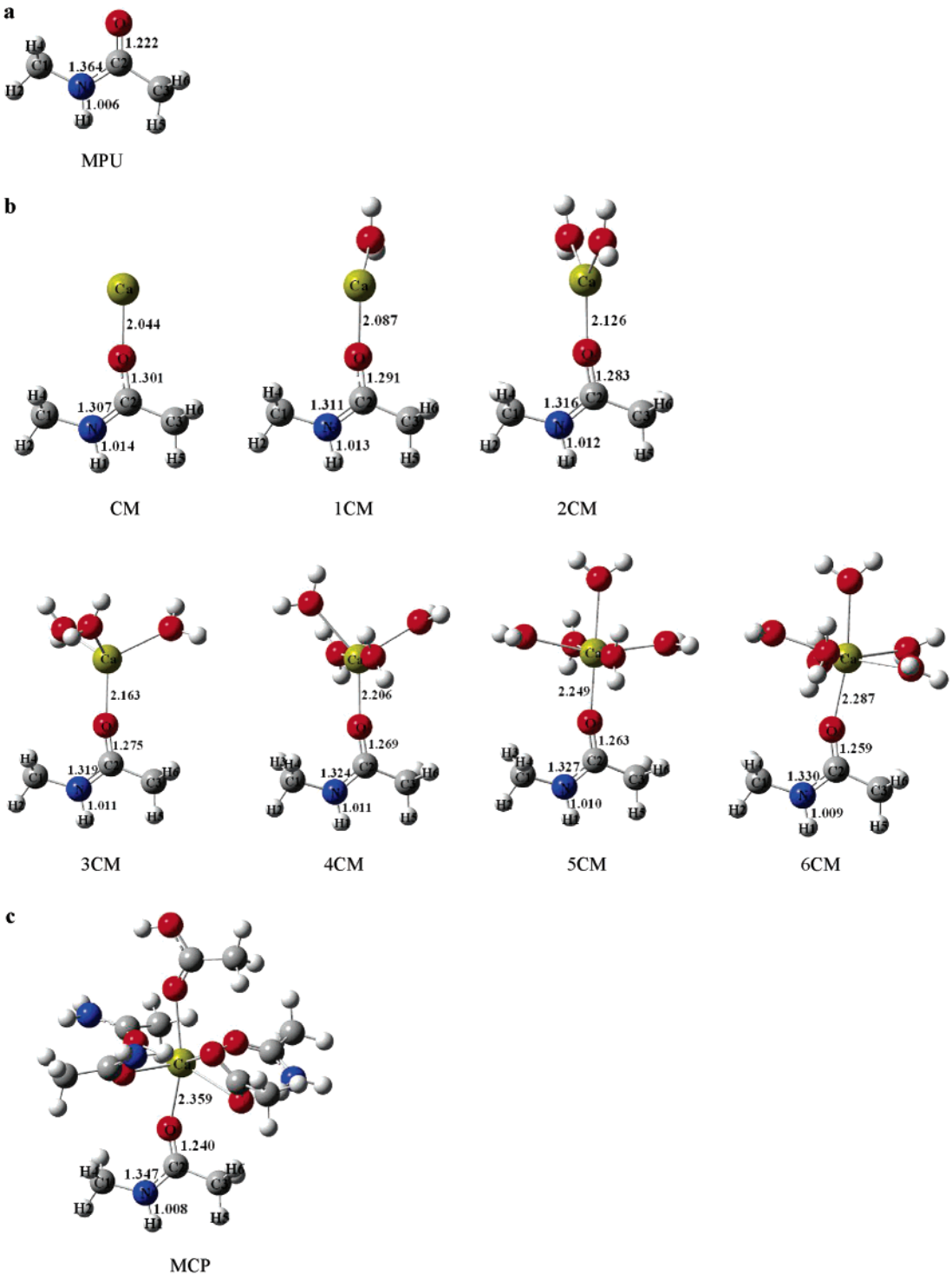

Figure 2. (a) Optimized modeling peptide unit (MPU) structure. (b) MPU interacting with bare or hydrated Ca^{2+} ion, forming CM or (1−6)CM. (c) The modeling calcium pump (MCP) structure. All of them are optimized at the B3LYP/6-311+G* level of theory.

are defined as the negative value of the Gibbs free energy changes and enthalpy changes, that is, GB = $-\Delta G$, PA = $-\Delta H$, respectively. Thus, the PA and GB are related by the entropy term: GB = PA + $T\Delta S$. Obviously, the larger the value of PA or GB is, the weaker the MH acidity is.[32]

Interaction energies between the MPU and Ca^{2+} ion are calculated using the supermolecule method,[33,34] which computes it as the difference between the energy for the cluster and those for the individual molecules that constitute it,

$$\Delta E_i = (E_N + E_{N'}) - E_M$$

where the subscript M refers to the total system, E_N indicates the optimized energy of the MPU Ca^{2+} ion, and $E_{N'}$ indicates the optimized energy for the fragment of the Ca^{2+} ion side. All of the energies discussed above are corrected by the zero-point vibrational energy (ZPVE) and the basis set superposition error (BSSE) corrections using the supermolecule method, where the BSSEs have been evaluated using the Boys−Bernardi counterpoise technique.[35]

The NMR isotropic shieldings σ(M) are calculated using the GIAO methods[36] with the B3LYP functional. The NMR shift $\delta(M) = \sigma(M)^{MPU} - \sigma(M)^{ion}$ is obtained as the shielding

TABLE 1: Selected Bond Distances (in Å) for the MPU, MPU Coordinated with Bare or Hydrated Ca^{2+} Ion, and the MCP as Well as the Corresponding Vibrational Frequencies (in cm^{-1})[a,b]

	MPU	CM	1CM	2CM	3CM	4CM	5CM	6CM	MCP
R(O−C)	1.222	1.301	1.291	1.283	1.275	1.269	1.263	1.259	1.240
Str(O−C)	1745	1566	1579	1591	1603	1611	1645	1648	1687
R(C−N)	1.364	1.307	1.311	1.316	1.319	1.324	1.327	1.330	1.347
Str(C−N)	1558	1675	1665	1655	1649	1643	1633	1612	1592
R(N−H)	1.006	1.014	1.013	1.012	1.011	1.011	1.010	1.009	1.008
Str(N−H)	3651	3578	3591	3600	3607	3614	3616	3621	3637
R(Ca−O)		2.044	2.087	2.126	2.163	2.206	2.249	2.287	2.359

[a] CM refers to the MPU coordinated with bare or hydrated Ca^{2+} ion, and the digital 1−6 before CM denotes the number of the water molecules coordinating with the Ca^{2+} ion. [b] Values obtained at the B3LYP/6-311+G* level of theory.

calculated for the MPU coordinating with the Ca^{2+} ion minus the shielding calculated in the MPU. The NMR spin−spin coupling constants ^nJ(A,B), where n is the number of bonds connecting nuclei A and B, are obtained using the coupled perturbed DFT method with the B3LYP functional. The J constants are calculated as a sum of the diamagnetic spin−orbit (DSO), paramagnetic spin−orbit (PSO), fermi contact (FC), and the spin dipolar (SD) contributions.[24,37]

The natural bond orbital (NBO) analysis[24,38] used for monitoring the sp^n hybrid character of the sigma bonding (σ), sigma antibonding (σ*), and lone pair (LP) orbitals in different complexes are also calculated for the discussed complexes using the DFT method with the B3LYP functional and 6-311+G* basis set.

All the calculations have been performed without any symmetry restricts using the Gaussian 03 packages.[39]

3. Results and Discussions

3.1. Geometric and IR Characters. The geometry and IR parameters of the MPU may change substantially when the carbonyl oxygen of the MPU occurs in direct interaction with the bare or the hydrated Ca^{2+} ion as well as when the MCP is formed. Figure 2a shows the optimized modeling peptide unit structure which is used as the reference system for comparison. The explicit structures of the MPU binding of the bare or the hydrated Ca^{2+} ion shown in Figure 2b are used to highlight the limiting case of the bare or the hydrated ion binding effect on the amide H of the MPU. The number of water molecules used to coordinate the Ca^{2+} ion on the first shell ranges from one to six to illustrate the situation when the coordination number of the Ca^{2+} ion is changed, though the strict coordination number is seven in biological systems. Optimized MCP shown in Figure 2c is used for the simulation of the situation which is close to the biological systems and is used for verification for our conclusion. The variation of the MPU geometrical parameters and the corresponding frequency shifts upon complexation at the carbonyl O with the bare or the coordinated Ca^{2+} ion are shown in Table 1, and the variation trends of the amide N−H bond of the MPU upon complexation are displayed in Figure 4 and demonstrate an intuitionistic effect. The results of the NBO analysis for each optimized structure are collected in Table 2.

As shown in Table 1, the amide N−H bond of the MPU is lengthened by about 0.08 Å upon binding of the bare Ca^{2+} ion, and the corresponding frequency red shift is 73 cm^{-1}. The variation of the N−H bond is reflected by the sp^n hybridization;[40] that is, the bond is weakened and elongated along with the increase of the p-character of the σ orbital. The (N−H) σ orbital of the MPU is the linear combination of the two orbitals localized at N and H. The calculated sp^n hybrid character 2.55 of the orbital localized at N in the MPU increases to 2.73 when the Ca^{2+} ion is coordinated to the O of the MPU. Moreover, the hybrid character of the (N−H) σ orbital is determined by the change of the orbital localized at the N because the orbital localized at the amide hydrogen is of 100% s-character in all complexes. Then the N−H bond of the MPU is lengthened when the bare Ca^{2+} ion is coordinated.

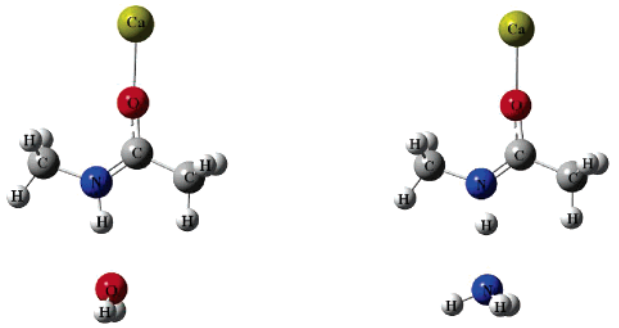

Figure 3. All of the structures illustrated in Figure 2 interact with H_2O and NH_3 forming the N−H···O or N−H···N hydrogen bindings. Here, we take these two structures combined with MPU and Ca^{2+} ion as examples for simplicity. All of these structures are optimized at the B3LYP/6-311+G* level of theory.

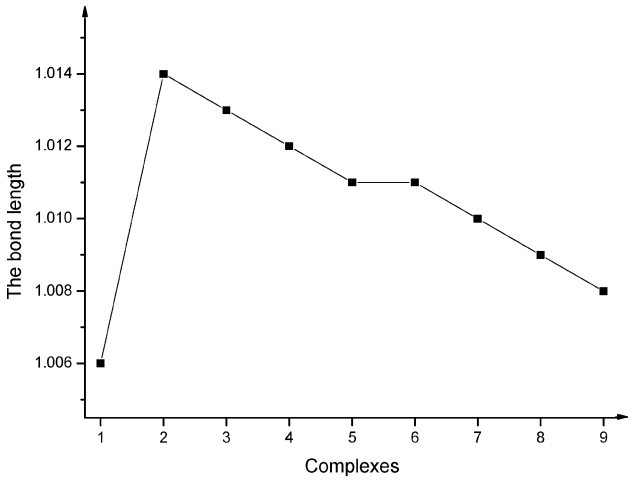

Figure 4. The changing trends of the N−H bond of the amide H in MPU and MPU interacting with bare or coordinated Ca^{2+} ion obtained at the B3LYP/6-311+G* level of theory. Here, **1** refers to the MPU monomer, **2** to **7** denote MPU interacting with bare and the 1−6 hydrated Ca^{2+} ions, respectively, and **9** refers to the MCP structure.

TABLE 2: NBO Analysis for the Selected Bonds of the MPU and MPU with Bare or Coordinated Ca^{2+} Ion[a,b,c]

	C−O(C)	C−O(O)	C−N(C)	C−N(N)	N−H(N)	N−H(H)
MPU	35.5%/2.03	64.5%/1.46	37.3%/2.19	62.7%/1.65	69.6%/2.55	32.5%
CM	32.7%/2.55	67.3%/1.42	38.3%/1.99	61.7%/1.57	71.9%/2.73	28.1%
1CM	33.0%/2.48	66.9%/1.41	38.2%/2.01	61.8%/1.58	71.7%/2.71	28.3%
2CM	33.3%/2.41	66.7%/1.40	38.2%/2.03	61.8%/1.59	71.6%/2.69	28.5%
3CM	33.6%/2.36	66.4%/1.40	38.1%/2.04	61.9%/1.59	71.4%/2.68	28.6%
4CM	33.9%/2.32	66.2%/1.39	38.1%/2.06	61.9%/1.60	71.2%/2.66	28.8%
5CM	34.1%/2.28	65.9%/1.40	38.0%/2.07	62.0%/1.60	71.1%/2.65	28.9%
6CM	34.3%/2.25	65.7%/1.41	37.9%/2.08	62.0%/1.61	71.0%/2.64	29.0%
MCP	33.9%/2.47	66.8%/1.68	37.6%/2.12	62.4%/1.59	70.0%/2.67	30.1%

[a] CM refers to the MPU coordinated with bare or hydrated Ca^{2+} ion, and the digital 1−6 before CM denotes the number of the water molecules coordinating with the Ca^{2+} ion. [b] The percentages in front of the slash refer to the calculated weight of the orbital localized at the atom in the bracket, and the data behind the slash refer to the sp^n hybridization of the orbital localized at the atom in the bracket. [c] Values calculated at the B3LYP/6-311+G* level of theory.

Additionally, the C−N bond of the MPU is lengthened and the carbonyl C═O bond is shortened if the MPU is coordinated with Ca^{2+} ion. This is ascertained by the corresponding frequency shifts. The frequency shifts of the C−N stretching modes in the ionized state of the MPU with respect to that in the monomer are 117 cm^{-1}, blue shift. Moreover, an 821 cm^{-1} red shift is observed for the carbonyl C═O stretching modes when the Ca^{2+} ion is coordinated with the MPU. Detailed NBO analysis of the (C−N) σ orbital unveils the increase of s-character of the orbital localized at the C1 as well as the N upon complexation. The sp^n hybridization of the orbital localized at the C1 is 2.03 and 2.55 in the MPU and the complex MPU···Ca^{2+}. The sp^n hybridization of the orbital localized at N is 1.65 and 1.57 for the same series of complex. Thus the s-character of the (C−N) σ orbital increases when the Ca^{2+} ion is coordinated with the MPU because the sp^n character of both orbitals localized at C1 and N of the MPU decreases simultaneously. However, a different situation is found for the sp^n character of the (C−O) σ orbital. The sp^n hybridization of the orbital localized at carbon amounts to 2.03 and 2.55 in the MPU and the complex MPU···Ca^{2+}. However, the sp^n hybridization of the orbital localized at oxygen decreases from 1.46 to 1.42 upon coordination of the Ca^{2+} ion to the MPU. The dominating part of the (C−O) σ orbital localized at oxygen is responsible for the decreasing of the double bond character of the MPU C═O bond because the calculated weight of the orbital localized at oxygen is increased by 64.5% and 67.3% for the MPU and the complex MPU···Ca^{2+}. This probably explains the bond elongation in complex MPU···Ca^{2+}.

The influence of the coordination with bare Ca^{2+} ion on the geometrical parameters and IR characters can also be found when the Ca^{2+} ion is hydrated as shown in Figure 2 and Table 1. The amide N−H and carbonyl O═C bonds are lengthened, and their corresponding frequencies are red-shifted, whereas the C−N bond of the MPU is shortened and the corresponding frequency is blue-shifted when the MPU is coordinated with the hydrated Ca^{2+} ion. All of these changes owing to the complexation with the hydrated Ca^{2+} ion can be explained from the calculated NBO parameters collected in Table 2, and we will not illustrate them one by one for simplicity here. From Figure 4, it can be seen intuitively that these variations of the N−H bonds are gradually decreased when the number of the water molecules which coordinate with the Ca^{2+} ion on the first shell is increased. This may be because of the complex capability or because the acidity of the Ca^{2+} ion is reduced along with the increase of the combination number around it. This can be seen from the distance between the Ca^{2+} ion and the carbonyl O of the MPU shown in Figure 2; that is, the Ca^{2+}···O is lengthened when the number of the water molecules combining with Ca^{2+} ion is increased.

Geometrical changes for the MPU can be also observed when the Ca^{2+} ion is coordinated with amino acid residues, that is, when the MCP is simulated. The amide N−H and carbonyl O═C bonds are lengthened, and the C−N bond of the MPU is shortened when the MCP is formed, which can be attributed to the redistribution of the electron cloud of the MPU caused by the emergence of the intramolecular Ca^{2+}···O bonding. These geometrical variations are ascertained by the corresponding IR characters and detailed NBO analysis collected in Tables 1 and 2. What is more important is that the same changes are ensured for us for the following discussions of the MPU with the bare or the hydrated Ca^{2+} ion.

3.2. NMR Parameters. The NMR spectroscopy parameters have been determined for the MPU base interacting with the bare or the coordinated Ca^{2+} ions. They are used for elucidating the influence of the Ca^{2+} ion binding on the amide H of the MPU motif. The magnitude of the net charge may influence NMR parameters significantly because of the polarization of molecular orbitals and the charge transfer between the Ca^{2+} ion and the MPU when the MPU is bounded by the Ca^{2+} ion with a net charge +2. All of the NMR parameters calculated at the B3LYP/6-311+G* level are listed in Table 3, and the variation trends of the NMR shieldings and the NMR shifts are displayed in Figure 5.

TABLE 3: NMR Parameters Including NMR Shieldings (in ppm), NMR Spin−Spin Couplings (in Hz), and NMR Shifts (in ppm) as Well as the Energy Gap between the σ and σ^*(N−H) Orbitals (in kcal/mol)[a,b]

	MPU	CM	1CM	2CM	3CM	4CM	5CM	6CM	MCP
NMR Shielding									
σ(H)	28.0	25.1	25.4	25.6	25.8	26.0	26.1	26.3	27.3
σ(N)	138.6	88.3	93.8	98.6	102.8	106.6	109.5	112.6	124.3
σ(O)	−84.0	29.5	40.0	42.4	39.3	33.0	26.5	18.0	−22.4
σ(C)	10.9	−6.7	−5.5	−4.5	−3.4	−2.5	−1.5	−1.0	2.5
σ(Ca)		1286.0	1232.1	1186.0	1164.4	1166.0	1167.4	1185.0	1159.7
NMR Spin−Spin Coupling									
J(N,H)	62.7	65.4	65.3	65.2	65.0	64.8	64.7	64.6	63.1
J(C,N)	10.9	15.4	15.0	14.6	14.3	13.9	13.7	13.5	13.0
J(O,C)	28.4	18.0	17.9	18.1	18.4	18.8	19.3	20.2	20.4
NMR Shift									
δ(H)	3.9	6.8	6.5	6.3	6.1	5.9	5.7	5.6	4.6
δ(N)	119.8	169.9	164.4	159.9	155.7	151.7	148.8	145.9	134.2
δ(C)	171.4	189.0	188.0	187.0	186.0	185.0	184.0	183.5	180.1
δ(O)	404.2	290.2	280.4	277.6	280.4	286.7	293.7	301.9	341.9
Energy Gap (Nitrogen−Hydrogen)									
σ-σ^*	674.2	667.5	669.1	670.1	670.7	671.6	672.0	672.4	669.0

[a] CM refers to the MPU coordinated with bare or hydrated Ca^{2+} ion, and the digital 1−6 before CM denotes the number of the water molecules coordinating with the Ca^{2+} ion. [b] Values calculated at the B3LYP/6-311+G* level of theory.

a. NMR Shieldings. As shown in Table 3, the calculated NMR shieldings σ(H1) and σ(N) of the MPU decrease (from 28.0 to 25.1 and from 138.6 to 88.3) upon the binding of the Ca^{2+} ion to the MPU. However, the NMR shielding σ(O) of the MPU is increased upon complexation with the bare Ca^{2+} ion (Table 3). This can be explained by the withdrawal of electron density from the carbonyl O of the MPU owing to the formation of the Ca^{2+}···O bonding between the Ca^{2+} ion and the carbonyl O of the MPU represented by the decrease of the calculated negative natural charge for oxygen (from −0.372 to −0.591) and the increase of the calculated negative natural charge for the amide N of the MPU (from −0.223 to −0.132) as well as the increase of the calculated positive charge for the amide H of the MPU (from 0.274 to 0.364). The decreased electronegativity at the amide nitrogen and the increased electronegativity at the oxygen of the MPU lead to the decrease of the calculated NMR shielding σ(H) or σ(N) and the increase of calculated NMR shielding σ(O) in cationized MPU. In other words, the polarization of the amide group in the MPU is decreased, and the interaction energy between the N and H atoms may reduce. That is to say, the proton countertransport of the amide H of the MPU may more easily occur when the bare Ca^{2+} ion is introduced.

Moreover, the electronegativity at the oxygen of the MPU is also increased because the introduction of the divalent cation with net charge +2 may lead the charge transfer between the ion and the MPU, and the net charge compensation of the divalent cation from the MPU base may occur. As a result, the electron density of the amide N and H are withdrawn by the carbonyl O of the MPU because the natural charge of oxygen

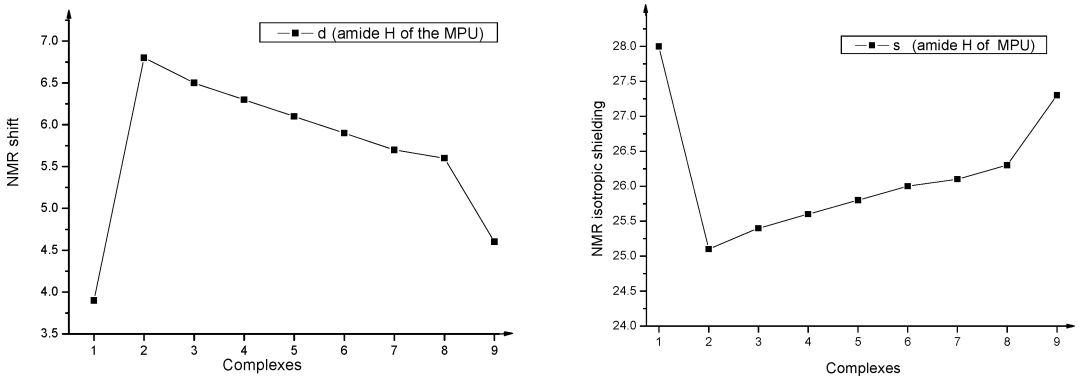

Figure 5. The changing trends of the NMR shielding and NMR shift of the amide H in MPU and MPU interacting with bare or coordinated Ca^{2+} ion obtained at the B3LYP/6-311+G* level of theory. Here, **1** refers to the MPU monomer, **2** to **7** denote MPU interacting with bare and the 1−6 hydrated Ca^{2+} ions, respectively, and **9** refers to the MCP structure.

is decreased further by contact with the Ca^{2+} ion. Then calculated NMR shieldings σ(H) and σ(N) are also decreased and the calculated NMR shielding σ(O) is increased when the Ca^{2+} ion interacting with the MPU is hydrated. However, these variations of the NMR shieldings are gradually decreased with the increase of the coordination number of water molecules around the Ca^{2+} ion because the interaction energy of the Ca^{2+}•••O bonding between the Ca^{2+} ion and the carbonyl O of the MPU is decreased when the coordination number is increased. This is also why the dependency of the NMR shieldings of the MPU between the MPU monomer and MCP is smaller than that between the MPU monomer and MPU coordinated with the bare or the hydrated Ca^{2+} ion, because of the strong coordinating capability of the amino acid residues compared with the water molecules. All of the data discussed above can be seen clearly in Table 3 and Figure 5.

b. NMR Shifts. The NMR shifts of the MPU due to the contact with the Ca^{2+} ion discussed in the text are calculated as a NMR shift of cationized MPU minus the NMR shift of the MPU monomer as shown in Table 3. The calculated upfield NMR shift δ(H1) of the MPU is 2.9 ppm upon the coordination of the bare Ca^{2+} ion. The same is true for the value of NMR calculated for the N of the cationized MPU state which shifts upfield by about 50.1 ppm. This can prove that the coordination with the bare Ca^{2+} ion is accompanied by further decrease of the electron density of amide H and nitrogen of the MPU. Similarly, the large NMR shift δ(O) of the MPU shifts downfield by −114.0 ppm upon the coordination of the ion and is accompanied by further decreases of the natural charge of oxygen which has been mentioned above.

In the same manner as the variation of the NMR shieldings, when the number of water molecules around the Ca^{2+} ion interacting with MPU is increased, the NMR shifts δ(H1), δ(N), and δ(O) are gradually decreased. Clearly this also can be explained by the fact that the interaction energy of the Ca^{2+}•••O bonding between the Ca^{2+} ion and the carbonyl O of the MPU is decreased when the coordinating number is increased. What is more important is that these variation trends of the NMR shifts δ(H1), δ(N), and δ(O) can also be obtained when the MCP simulated though the electron withdrawing of the amino acid residues is larger than water molecules which induce the weakening of the Ca^{2+}···O bonding between the Ca^{2+} ion and the carbonyl O of the MPU. The analysis of the calculated NMR shielding σ or NMR shifts δ of amine H in the MPU reveals that the electron density as well as the polarization of the amide N−H bond of the MPU is decreased. That is to say, the N−H bond of the MPU is weakened when the calcium pump structure is formed.

c. NMR Couplings. As shown in Table 3, the calculated NMR spin−spin coupling constant ^1J(C2, O) of the MPU decreases by 10.4 Hz upon the interaction of the MPU with the bare Ca^{2+} ion. The calculated SD, PSO, and DSO contributions to the ^1J(C2, O) coupling are 0.1, 0.6, and zero, respectively. They are much smaller compared with the FC term of the ^1J(C2, O) coupling which is decreased from 17.0 to 9.8 Hz. Then, the decrease of the coupling constant ^1J(C2, O) is driven by the FC contribution. Since the magnitude of the FC term is known to affect the s-electrons at the sites of coupled nuclei, the s-character decrease of the (C2, O) σ orbital which has been mentioned above explains the decrease of the FC contribution of the ^1J(C2, O) coupling. The same is true for the NMR spin−spin coupling constant ^1J(C2, N) of the MPU. The NMR spin−spin coupling constant ^1J(C2, N) increase of 4.5 Hz upon the binding of the MPU with the bare Ca^{2+} ion can be explained by the s-character of the (C2, N) σ orbital giving rise to the FC contribution which is changed from 13.0 to 18.4 Hz, whereas the variation of the calculated SD, PSO, and DSO terms which are 0.7, −1.5, and zero, respectively, are much smaller than the FC contribution when the MPU is bounded with Ca^{2+} ions.

However, something is different for the calculated NMR spin−spin coupling constant ^1J(N, H) of the MPU. As mentioned above, the NBO analysis indicates that the s-character of the (N, H) σ orbital is decreased which should give rise to the decreasing of the FC contribution. However, the calculated ^1J(N, H) coupling constant increases from 62.7 to 65.4 Hz because the increase of the FC contribution in the MPU is increased by 3.4 Hz upon the binding of the Ca^{2+} ion to the MPU. This may be because the changes of the FC term are explained on the basis of the calculated sp^n hybrid character of σ bonding, σ* antibonding, and lone pair orbitals and by considering the energy gap between the orbitals in different complexes.[24] The increasing of the FC term is caused mainly by the decrease of the energy gap between the σ and σ* (nitrogen−hydrogen) orbitals (viz., 6.7 kcal/mol) rather than by the change of the s-character of the (N, H) σ orbitals.

Moreover, the variations of the NMR spin−spin coupling constants ^1J(C2, O), ^1J(C2, N), and ^1J(N, H) of the MPU are smoothly decreased when the coordination numbers around the Ca^{2+} ion interacting with the MPU are increased because of the decreased interaction energies of the Ca^{2+}···O bonding between the Ca^{2+} ion and the carbonyl O of the MPU. These variations of the NMR spin−spin coupling constants when the MCP is simulated are smaller than those between the MPU monomer and the MPU coordinated with hexahydrated Ca^{2+} ion because of the strong coordinating capability of the amino acid residues compared with the water molecules.

TABLE 4: GB and PA Parameters Calculated for the Discussion of the Acidity of the Amide N−H of MPU and the Interaction Energy between the Ca^{2+} Ion and the MPU Base[a,b]

	MPU	CM	1CM	2CM	3CM	4CM	5CM	6CM	MCP
$-\Delta H$	358.6	169.2	179.9	189.0	197.1	202.6	208.0	211.0	306.5
$-\Delta G$	360.5	169.3	180.3	188.7	195.0	206.5	212.0	217.0	333.9
E_i		108.3	92.0	79.7	67.8	54.4	46.5	32.1	13.1

[a] CM refers to the MPU coordinated with bare or hydrated Ca^{2+} ion, and the digital 1−6 before CM denotes the number of the water molecules coordinating with the Ca^{2+} ion. [b] Values obtained at the B3LYP/6-311+G* level of theory.

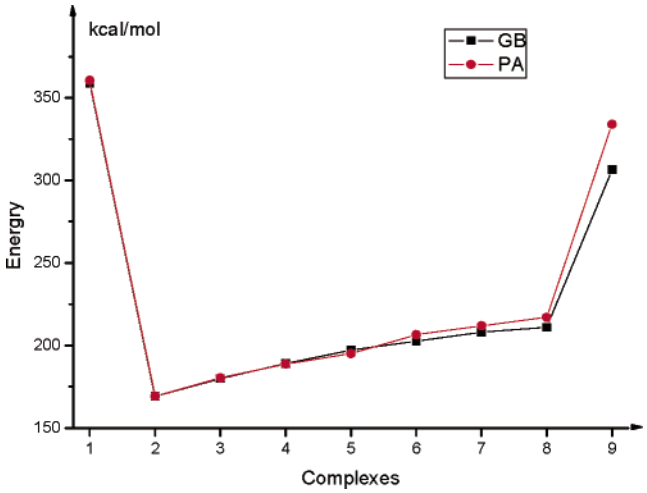

Figure 6. The changing trends of the acidity of the amide H in MPU induced with bare or coordinated Ca^{2+} ion interacting with carbonyl O of MPU. Here, **1** refers to the MPU monomer, **2** to **7** denote MPU interacting with bare and the 1−6 hydrated Ca^{2+} ions, respectively, and **9** refers to the MCP structure.

3.3. Acidity Aspect. Acidity of the amide H of the MPU is discussed in the text to investigate the effect of the coordination with Ca^{2+} ion on the activity of the proton H of the amide in the MPU. As mentioned above, GB and PA are used to probe the acidity in this section. All of the calculated GB and PA for amide H of the MPU and MPU interacting with the bare or the coordinated Ca^{2+} ions are collected in Table 4. The variation trends of GB and PA with the coordination number of Ca^{2+} ion are displayed in Figure 6.

Calculated results show that GB and PA decrease from 358.6 to 169.2 kcal/mol and from 360.5 to 169.3 kcal/mol, respectively, when MPU is coordinated with the bare Ca^{2+} ion. That is to say, the amide H of the MPU is easy to lose when the Ca^{2+} ion combines to the carbonyl O of the MPU, which can be attributed to the weakening of the amide N−H bond by the appearance of the intramolecular $Ca^{2+}\cdots$O bonding. The same is true for the situation that Ca^{2+} ion is hydrated or coordinated with amino acid residues. Moreover, as displayed in Table 4, the effect of Ca^{2+} ion on the acidity of the amide H of the MPU is gradually decreased along with the increase of the coordination number of water molecules due to the weakening of the intramolecular $Ca^{2+}\cdots$O bond. Although the electron-withdrawing of the carbonyl O of the amino acid residues is larger than that of the O of the water molecule, the acidity of the amide H of the MPU in MCP is also increased as expected.

The interaction energies of the $Ca^{2+}\cdots$O bonding versus GB are presented in Figure 7. From their linear relationship, we can conclude that the influence of the Ca^{2+} ion on the activity of the amide H in the MPU is larger when the acidity of the

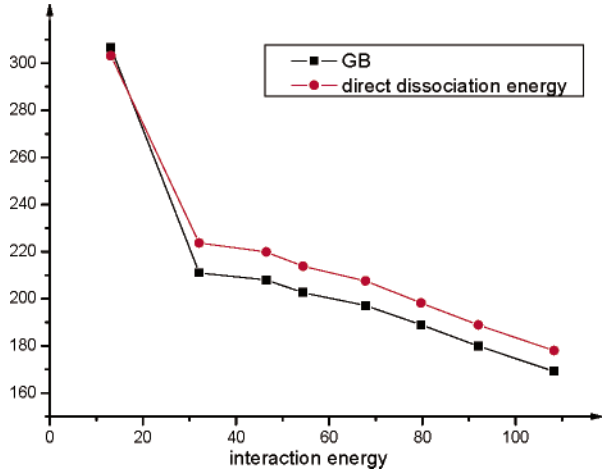

Figure 7. Plot of the interaction energies of the $Ca^{2+}\cdots$O bonding versus the values of GB and the direct dissociation energies of the amide H in MPU (in kcal/mol).

Ca^{2+} ion is stronger because the interaction energy can be seen as the index for the acidity of Ca^{2+} ion.

From the results of the acidity of the amide H in MPU illustrated above, we can obtain that the proton H of the amide is easy to lose when the MPU is coordinated with the bare or the hydrated Ca^{2+} ion even if the calcium pump structure is formed.

3.4. Assisting Proton Dissociation. All of the results discussed above have proved that the amide H is activated when the calcium pump is formed. It is known that in the helical peptide linkage structure N−H$\cdots$O=C hydrogen bonds exist possessing proton donor and acceptor groups. Therefore, we can predict that the proton transfer will happen easily if there are stronger electron-withdrawing groups, such as carbonyl O of the peptide linkage forming a hydrogen bond with the amide H of the calcium pump structure. To verify our prediction, NH_3 and H_2O are used as the assisting groups for the dissociation of the amide H in MPU. Moreover, the dissociation energy for the deprotonation process of the amide H of the MPU displayed in Figure 3 is discussed for the purpose of the comparison of the assisted dissociation effect of the H_2O and NH_3 molecules though it corresponds to the acidity of the proton. All of the calculated dissociation energies are listed in Table 5. The variation trends of the dissociation energies with the assisting of NH_3 and H_2O molecules and those of the cases with the increase of the coordination number of Ca^{2+} ion are displayed in Figure 8.

The dissociation energy for the direct deprotonation process of the amide H in MPU is about 358.0 kcal/mol. Further, it is lowered by about 195.6 and 154.6 kcal/mol when the NH_3 and H_2O molecules are used as the assisting dissociation group, and the effect of the former is clearly larger than the latter because of the higher basicity of the NH_3 compared with the H_2O molecule. The dissociation energy of the direct deprotonation process of amide H of MPU coordinated with Ca^{2+} ion which is about 178.0 kcal/mol is lower than that for the MPU monomer by about 180.0 kcal/mol because of the effect of the Ca^{2+} ion on the acidity of the amide H of the MPU. Similarly, the assisted dissociation energy for the amide H of the $Ca^{2+}\cdots$MPU is decreased by about 188.8 and 149.7 kcal/mol, respectively, when the NH_3 and H_2O molecules are used as the assisting groups.

As shown in Figure 7, it can be obtained that the dissociation energy for the direct dissociation processes of the amide H of the MPU is gradually increased when the number of the coordinated water molecules is increased because of the

TABLE 5: Dissociation Energy and Assisted Dissociation Energy for the Deprotonation Processes of Proton Dissociating from the Amide N of the MPU or Ca^{2+} Ionized MPU[a,b]

	MPU	CM	1CM	2CM	3CM	4CM	5CM	6CM	MCP
direct	358.0	178.0	188.9	198.2	207.6	213.8	219.9	223.7	303.1
NH_3 assisted	162.4	−10.8	−1.7	6.1	14.3	19.7	24.9	28.2	102.4
H_2O assisted	203.4	28.3	37.9	45.9	54.4	59.8	65.2	69.1	143.0

[a] CM refers to the MPU coordinated with bare or hydrated Ca^{2+} ion, and the digital 1−6 before CM denotes the number of the water molecules coordinating with the Ca^{2+} ion. [b] Values obtained at the B3LYP/6-311+G* level of theory.

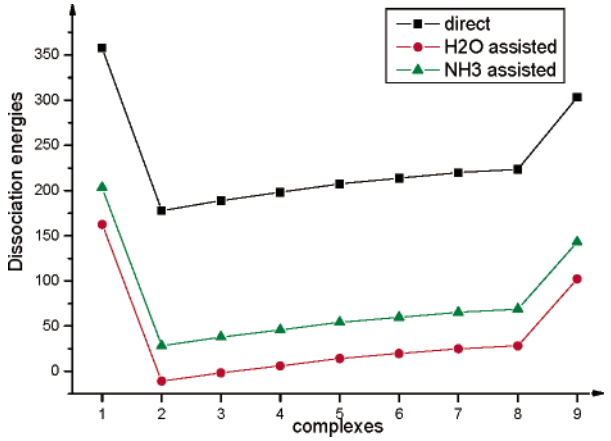

Figure 8. The changing trends of the direct and NH_3 and H_2O assisted dissociation energies of the amide H in MPU and MPU with the bare or coordinated Ca^{2+} ion. Here, **1** refers to the MPU monomer, **2** to **7** denote MPU interacting with bare and the 1−6 hydrated Ca^{2+} ions, respectively, and **9** refers to the MCP structure.

weakening of the intramolecular $Ca^{2+}\cdots O$ bond. In other words, the stronger the acidity of the Ca^{2+} ion is, the smaller the direct dissociation energy is. The same is true for the assisted case by the NH_3 or H_2O molecules. All of those confirm our prediction that the proton transfer may happen if there is a strong electron-withdrawing group such as a carbonyl O group forming N−H···O═C hydrogen bonds with the amino H of the MPU when the calcium pump is formed.

4. Conclusions

In the present study, for the purpose of validating the ionization states of the acidic residues forming the Ca^{2+}-binding sites that may transport protons of the peptide in the direction opposite to Ca^{2+}, the property changes of the amide H in the MPU due to the contact with Ca^{2+} ion have been investigated at the B3LYP/6-311+G* level of theory. The relevant geometries, NMR parameters, acidity of the amide H of MPU, and the assisted dissociation energies have been discussed, respectively. The principal conclusions from this study are described as follows:

(1) The amide N−H bond of the MPU is lengthened by about 0.08 Å and the corresponding vibration is red-shifted by 73 cm^{-1} because the calculated sp^n hybrid character 2.55 of the orbital localized at nitrogen in the MPU increases to 2.72 when Ca^{2+} ion binds to the oxygen of MPU.

(2) Calculated NMR shielding σ(H1) of the MPU shifts upfield 2.8 ppm upon complexation with the bare Ca^{2+} ion. This may be attributed to the fact that the coordination with the bare Ca^{2+} ion causes further decrease of electron density of the amide H of the MPU as represented by the natural charge for amide H of the MPU, increased from 0.274 to 0.364 e.

(3) Calculated results show that GB and PA are decreased from 359.9 to 169.0 kcal/mol and from 357.91 to 168.7 kcal/mol, respectively, when the MPU is bounded by the bare Ca^{2+} ion. That is to say, the amide H of the MPU is easy to lose when the Ca^{2+} ion combines to the carbonyl O of the MPU.

(4) Dissociation energy for the direct deprotonation process of the amide H in the MPU is reduced by about 195.6 and 154.6 kcal/mol, respectively, in the NH_3 and H_2O assisted cases. Further, they are about 188.8 or 149.7 kcal/mol when the MPU is bounded with the Ca^{2+} ion.

(5) All of the changes for the parameters discussed above for the amide H of the MPU can also be obtained when the Ca^{2+} ion is coordinated with water molecules or amino acid residues. Moreover, when the acidity of the coordinated Ca^{2+} ion is stronger, the influence of the Ca^{2+} ion on the activity of the proton H of the amide in the MPU is larger because the interaction energy can be seen as the index for the acidity of the Ca^{2+} ion. All of these results confirm our prediction that the amide H of the MPU is activated and may be transported in the direction opposite to the Ca^{2+} when the calcium pump is formed.

Acknowledgment. This work is supported by NSFC (Grant No. 20573063 and Grant No. 20273040), NIH(Grant No. GM62790), NCET and the NSF of Shandong Province (Z2003B01), SRFD, SCF for ROCS-SEM, and the project of ChinaGrid. Support from Virtual Laboratory for Computational Chemistry of CNIC and Supercomputing Center of CNIC-CAS is also acknowledged. A part of calculations were performed on the Center for Biological Modeling and the Michigan Center for Biological Information Linux clusters at Michigan State University, and the High-Performance Computational Center in Shandong University. The author (Y.B.) also thanks Prof. Yi Hu for his help in calculations.

References and Notes

(1) Yuji, S.; Naoyuki, M.; Mitsunori, L.; Akinori, K.; Chikashi, T. *J. Am. Chem. Soc.* **2004**, *127*, 6150.
(2) Toyoshima, C.; Nakasako, M.; Nomura, H.; Ogawa, H. *Nature* **2000**, *405*, 647.
(3) Meldolesi, J.; Pozzan, T. *Trends Biochem. Sci.* **1998**, *23*, 10.
(4) Tsien, R. W.; Tsien, R. Y. *Annu. Rev. Cell Biol.* **1990**, *6*, 715.
(5) Youxing, J.; Alice, L.; Jiayun, C.; Martine, C.; Brian, T. C.; Roderick, M. *Nature* **2002**, *417*, 515.
(6) Berridge, M. J.; Lipp, P.; Bootman, M. D. *Nat. Rev. Mol. Cell Biol.* **2000**, *1*, 11.
(7) Carafoli, E.; Santella, L.; Brance, D.; Brisi, M. G. *Crit. Rev. Biochem. Mol. Biol.* **2001**, *36*, 107.
(8) Michael, J. B.; Martin, D. B.; Llewelyn, B. H. *Nature* **2003**, *4*, 517.
(9) Michael, T. H.; John, D. L.; Sayeh, A. *Biochemistry* **2000**, *39*, 5859.
(10) Møller, J. V.; Juul, B.; le Maire, M. *Biochim. Biophys. Acta* **1996**, *1286*, 1.
(11) Lee, A. G.; East, J. M. *Biochem. J.* **2001**, *356*, 665.
(12) Toyoshima, C.; Nomura, H. *Nature* **2002**, *418*, 605.
(13) Xu, C.; Rice, W. J.; He, W.; Stokes, D. L. *J. Mol. Biol.* **2002**, *316*, 201.
(14) Maclennan, D. H.; Brandl, C. J.; Korczak, B.; Green, N. M. *Nature* **1985**, *316*, 696.
(15) Ebashi, S.; Lipman, F. *J. Cell. Biol.* **1962**, *14*, 389.
(16) Moller, J. V.; Juul, B.; Maire, L. M. *Biochim. Biophys. Acta* **1996**, *1286*, 1.
(17) Maclennan, D. H.; Rice, W. J.; Green, N. M. *J. Biol. Chem.* **1997**, *272*, 28815.
(18) Mcintosh, D. B. *Adv. Mol. Cell. Biol.* **1998**, *23A*, 33.

(19) Toyoshima, C.; Mizutani, T. *Nature* **2004**, *430*, 529.
(20) Toyoshima, C.; Nomura, H.; Tsuda, T. *Nature* **2004**, *432*, 361.
(21) Sørensen, T. L. M.; Møller, J. V.; Nissen, P. *Science* **2004**, *304*, 1672−1675.
(22) Hoeflich, K. P.; Ikura, M. *Cell* **2002**, *108*, 739.
(23) Petrov, A. S.; Lamm, G.; Pack, G. R. *J. Phys. Chem. B* **2002**, *106*, 3294.
(24) Sychrovsky, V.; Sporer, J.; Hobza, P. *J. Am. Chem. Soc*. **2004**, *126*, 663.
(25) Dingley, A. J.; Grzesiek, S. *J. Am. Chem. Soc*. **1998**, *120*, 8293.
(26) Szilagyi, L. *Prog. Nucl. Magn. Reson. Spectrosc*. **1995**, *27*, 325.
(27) Williamson, M. P.; Asakura, T. *Methods Mol. Biol*. **1997**, *60*, 53.
(28) Case, D. A. *Curr. Opin. Struct. Biol*. **2000**, *10*, 197.
(29) Wishart, D. S.; Case, D. A. *Methods Enzymol*. **2001**, *338*, 3.
(30) Clarke, D. M.; Loo, T. W.; Inesi, G.; MacLennan, D. H. *Nature* **1989**, *339*, 476.
(31) Florence, C.; Michael, B.; Stephan, G. *J. Am. Chem. Soc*. **2003**, *125*, 15750.
(32) Li, P.; Bu, Y. X.; Ai, H. Q.; *J. Phys. Chem. A* **2004**, *108*, 4069.
(33) Hobza, P.; Zahradnik, R. *Intermolecular Complexes;* Elsevier: Amsterdam, The Netherlands, 1988.
(34) Lenthe, J. H.; Duijneveldt-van de Rijdt, J. G. C. M.; Duijneveldt, F. B. *Adv. Chem. Phys*. **1987**, *521*, 124.
(35) Boys, S. F.; Bernardi, F. *Mol. Phys.* **1970**, *553*, 19.
(36) (a) Ditchfield, R. *Mol. Phys*. **1974**, *27*, 789. (b) Dodds, J. L.; McWeeny, R.; Sadlej, A. J. *Mol. Phys*. **1980**, *41*, 1419. (c) Wolinski, K.; Hilton, J. F.; Pulay, P. *J. Am. Chem. Soc*. **1990**, *112*, 8251.
(37) Ramsey, N. F. *Phys. Rev*. **1953**, *91*, 303.
(38) Reed, A. E.; Curtiss, L. A.; Weinhold, F. *Chem. Rev.* **1988**, *88*, 899.
(39) Frisch, M. J.; Trucks, G. W.; Schlegel, H. B.; Scuseria, G. E.; Robb, M. A.; Cheeseman, J. R.; Montgomery, J. A., Jr.; Vreven, T.; Kudin, K. N.; Burant, J. C.; Millam, J. M.; Iyengar, S. S.; Tomasi, J.; Barone, V.; Mennucci, B.; Cossi, M.; Scalmani, G.; Rega, N.; Petersson, G. A.; Nakatsuji, H.; Hada, M.; Ehara, M.; Toyota, K.; Fukuda, R.; Hasegawa, J.; Ishida, M.; Nakajima, T.; Honda, Y.; Kitao, O.; Nakai, H.; Klene, M.; Li, X.; Knox, J. E.; Hratchian, H. P.; Cross, J. B.; Bakken, V.; Adamo, C.; Jaramillo, J.; Gomperts, R.; Stratmann, R. E.; Yazyev, O.; Austin, A. J.; Cammi, R.; Pomelli, C.; Ochterski, J. W.; Ayala, P. Y.; Morokuma, K.; Voth, G. A.; Salvador, P.; Dannenberg, J. J.; Zakrzewski, V. G.; Dapprich, S.; Daniels, A. D.; Strain, M. C.; Farkas, O.; Malick, D. K.; Rabuck, A. D.; Raghavachari, K.; Foresman, J. B.; Ortiz, J. V.; Cui, Q.; Baboul, A. G.; Clifford, S.; Cioslowski, J.; Stefanov, B. B.; Liu, G.; Liashenko, A.; Piskorz, P.; Komaromi, I.; Martin, R. L.; Fox, D. J.; Keith, T.; Al-Laham, M. A.; Peng, C. Y.; Nanayakkara, A.; Challacombe, M.; Gill, P. M. W.; Johnson, B.; Chen, W.; Wong, M. W.; Gonzalez, C.; Pople, J. A. *Gaussian 03*, revision B.05; Gaussian, Inc.: Wallingford, CT, 2004.
(40) Alabugin, I. V.; Manoharan, M.; Peabody, S.; Weinhold, F. *J. Am. Chem. Soc*. **2003**, *125*, 5973.